Dynamic light scattering at induced oscillations of particles of polydisperse liquid-droplet aerosol as applied to determination of aerosol particle size spectrum

A.A. Zemlyanov, Yu.E. Geints, and A.V. Pal'chikov

Institute of Atmospheric Optics,
Siberian Branch of the Russian Academy of Sciences, Tomsk

Received May 6, 2000

The frequency dependence of the intensity of the dynamic component of light scattered at induced (ponderomotive) oscillations of particles of a polydisperse liquid-droplet aerosol is calculated numerically. Based on a solution of the inverse problem by the method of histograms, it is shown that the particle size distribution function can be reconstructed with sufficient accuracy.

Introduction

Oscillating liquid particles change their shape, and this leads to appearance of the dynamic component in the radiation scattered by the aerosol. These oscillations can be caused by the particle motion in the atmosphere or stimulated by radiation. The natural oscillation frequencies of droplets are unambiguously determined both by their size and physical–chemical properties of the liquid. Therefore, the numerical information on the aerosol size distribution function can be derived from the frequency behavior of the dynamic component of the scattering.

The possibility of practical use of the electromagnetic (UHF) radiation modulated at oscillating droplets for determining the size of rain droplets was discussed in Ref. 1. In that paper devoted to experimental study of fluctuations of a radar echo from clouds, Brook and Latham noted the necessity of taking into account the random phase in the electromagnetic radiation scattering by arbitrarily oriented particles. In Ref. 2, the same authors conducted laboratory measurements of the variable component of intensity of the UHF radiation scattered at oscillations of individual droplets (diameter ~ 0.3–0.5 cm) blown by the air flow. Light scattering by rain droplets (diameter ~ 0.1–0.3 cm) illuminated from below by a searchlight was studied in Ref. 3. Light scattered by droplets was recorded by a photo camera as a series of bright bursts (tracks). The diameter of a droplet was derived from the burst repetition period, and then the size distribution was constructed for all droplets falling in the camera's field of view.

Under exposure of a droplet to high-power laser radiation, its surface is deformed due to ponderomotive forces. The theoretical principles of this effect are considered in Ref. 4. Exposing a particle to modulated laser radiation and changing its modulation frequency, it is possible to initiate oscillations of various groups of particles of a certain size.[5] The frequency dependence of the intensity of light scattered at induced oscillations of aerosol particles was obtained experimentally in Ref. 6, but, unfortunately, the reconstruction of the aerosol size distribution function has not been performed there.

Resonant build-up of droplet oscillations leads to increasing the amplitude of the dynamic component of the scattered radiation. Besides, the use of the modulated pumping radiation results in co-phase oscillations of droplets. This, in its turn, leads to better detection of the dynamic component of the scattered radiation as compared to spontaneous oscillations of droplets. In Refs. 7 and 8, the resonant build-up and dynamic scattering of light at ponderomotive oscillations of surfaces of individual droplets having arbitrary sizes were studied theoretically.

In this paper, the scattering by a group of oscillating particles is numerically simulated, and the possibility to derive the particle size distribution function from the dynamic component of the scattered radiation is considered.

Fundamental equations for calculating ponderomotive oscillations of transparent droplets and dynamic component of intensity of scattered radiation

The general statement of the problem on deformation of a liquid transparent droplet in a light field is given in Refs. 6–9. It includes the equations of dynamics of incompressible liquid formulated with allowance made for the action of ponderomotive forces. The equation describing the spatial-temporal evolution of deformations of the droplet surface is the equation of induced oscillations of a low-viscosity liquid for the coefficients of expansion of a particle surface displacement in terms of spherical harmonics:

0235-6880/00/09 777-05 $02.00

$$\frac{d^2 \xi_l}{dt^2} + \frac{2}{t_l}\frac{d\xi_l}{dt} + \Omega_l^2 \xi_l = \frac{l f_l(t)}{a_0 \rho_a}. \quad (1)$$

The radius of a deformed particle is described by the equation

$$a(t, \theta) = a_0 + \xi(t, \theta) = a_0 + \mathrm{Re}\left\{\sum_{l=2}^{\infty} \xi_l(t)\ Y_{l0}(\theta)\right\},$$

where ξ_l are the expansion coefficients of a surface displacement; a_0 is the radius of the unperturbed particle; $Y_{l0}(\theta)$ are spherical harmonics; θ is the polar angle; $t_l = a_0^2/[2(2l+1)(l-1)\nu]$ is the characteristic time of oscillation damping due to the effect of viscous forces; $\nu = \eta/\rho_a$ is the kinematical viscosity of the liquid;

$$\Omega_l = \sqrt{l(l+2)(l-1)\sigma/(\rho_a a_0^3)} \quad (2)$$

are the natural frequencies of droplet oscillations; σ, ρ_a, and η are the surface tension coefficient, density, and dynamic viscosity of the liquid, respectively.

The right-hand side of Eq. (1) describes the "inducing" force

$$f_l(t) = \int_0^{\pi} f(t, \theta)\ Y_{l0}^*(\theta) \sin\theta\, d\theta,$$

where $f(t, \theta) = (\varepsilon_a - 1)/(8\pi)[(\varepsilon_a - 1)(\mathbf{E}(t, \theta)\,\mathbf{n})^2 + E^2(t, \theta)]$ is the change of the normal component of tension of the electric field on the droplet surface[10]; ε_a is the permittivity of the droplet matter; $E(\theta)$ is the strength of the electric field on the droplet surface; $\mathbf{n}$ is the vector of the external normal to the particle surface.

The coefficients f_l depend on the electric field distribution on the droplet surface. As is well-known, for large particles this distribution has a sharply inhomogeneous structure, and therefore f_l can be determined only numerically.

Oscillating particles are scatterers with the dynamically varying shape of the surface. Obviously, the intensity of light scattered by such particles also experiences oscillations in time. As was shown in Ref. 8, for small perturbations of the droplet surface $|\xi| \ll a_0$, the intensity of the scattered radiation can be presented as a sum, in which the first term determines the elastic scattering by unperturbed droplet, and other terms are responsible for the contribution to light scattering at Raman frequencies:

$$I_s(\mathbf{r}, t) = \frac{c\sqrt{\varepsilon_a}}{8\pi}\mathbf{E}_s(\mathbf{r}, t)\,\mathbf{E}_s^*(\mathbf{r}, t) \approx$$

$$\approx \frac{c\sqrt{\varepsilon_a}}{8\pi}\left(\frac{k^2(\varepsilon_a - 1)}{4\pi r}\right)^2 \left[T(t)\,T^*(t) + \right.$$

$$+ T^*(t)\, a_0^2 \int \mathbf{E}(a_0, \theta', t) \exp\{ik\mathbf{r}' \cos\gamma_1\} \times$$

$$\left. \times \mathrm{Re}\left\{\sum_l \xi_l(t)\ Y_{l0}(\theta')\, do'\right\} + T(t)\, a_0^2 \int \mathbf{E}^*(a_0, \theta', t) \times \right.$$

$$\left. \times \exp\{-ik\mathbf{r}' \cos\gamma_1\} \mathrm{Re}\left\{\sum_l \xi_l(t)\ Y_{l0}(\theta')\, do'\right\}\right], \quad (3)$$

where

$$T(t) = \int_{V_{a_0}} \mathbf{E}(\mathbf{r}', t) \exp\{ik\mathbf{r}' \cos\gamma_1\}\, d\mathbf{r}';$$

k is the wave number; γ_1 is the angle between the vectors $\mathbf{r}$ and $\mathbf{r}'$.

As the modulation frequency Ω of the acting radiation changes, every burst of the scattered radiation corresponds to resonant build-up of mechanical oscillations of particles of a certain size. The square dependence of I_s on a_0 shows that as the particle size increases, the contribution of this particle to the intensity of the scattered radiation increases too.

Angular dependence of intensity of the scattered radiation was calculated numerically by Eq. (3). It has shown that the relative change of the intensity with respect to unperturbed (elastic) scattering at the frequencies of mechanical oscillations of a droplet is maximum in the direction normal to the action ($\theta = 90°$) and in the direction of the primary-rainbow angle ($\theta \approx 137°$). This determines the angles of optimal reception of the dynamic component of the scattered radiation.

Reconstruction of the aerosol particle size distribution function

Let us estimate the possibility of reconstructing the aerosol particle size distribution function using the following assumptions. We believe that all particles in the sensed aerosol volume V are under the same power conditions. This implies that the intensity of radiation incident on particles is the same and the angle to the receiver is roughly the same too. Then, obviously, the intensity I of the radiation scattered by the aerosol in the single-scattering approximation is

$$I(\Omega) = N_0\, V \int_0^{\infty} I_s(a_0, \Omega)\, f(a_0)\, da_0, \quad (4)$$

where N_0 is the concentration of droplets; $f(a_0)$ is the normalized particle size distribution function; Ω is the modulation frequency of the acting radiation; I_s is the intensity of scattering by a single particle.

It is readily seen that Eq. (4) is the Fredholm equation of the first kind. It can be solved using some standard method, for example, the method of histograms.[11] In this method, the area under curve is replaced by rectangles, and the integral is transformed into a sum:

$$I(\Omega) = N_0 V \sum_{i=1}^{n} N_{i,i+1}\, I_s^{i,i+1}\, \Delta a_0,$$

where $N_{i,i+1}$ is the relative concentration of particles with the sizes falling in the range i, $i+1$, whose width is equal to Δa_0; $I_s^{i,i+1}$ is the intensity of radiation scattered by a single particle from this range (the

particle size is usually assumed to correspond to the range center). Let us consider the situation in which particles of only certain sizes corresponding to the centers of intervals are in the selected volume. The total intensity of the radiation emitted by this volume is a sum of intensities scattered by individual particles:

$$I = N_0 V \sum_{i=1}^{n} N_i I_s^i, \quad (5)$$

where N_1, ..., N_n are the relative concentrations of particles of a certain radius; I_s^1, ..., I_s^n are the intensities of the radiation scattered by every droplet of the given size.

The intensity of the pumping radiation is modulated at several frequencies chosen resonant to every chosen particle size. For each modulation frequency Ω_j, we can write analytical equations similar to Eq. (5). Consequently, for several frequencies we have a set of algebraic equations:

$$I(\Omega_j) = N_0 V \sum_{i=1}^{n} N_i I_s^i(\Omega_j), \quad (6)$$

where Ω_1, ..., Ω_n are the natural resonance frequencies of mechanical oscillations of droplets with radii a_1, ..., a_n.

Figure 1 shows frequency dependence of the amplitude of steady oscillations for particles of different sizes. Just such a behavior causes the dependence $I_s^n(\Omega)$. The monotonic dependence of the resonant curve maximum on the particle radius is clearly seen in the figure. The dependence of the maximum surface displacement for droplets of different sizes and some their oscillation modes (fundamental mode $l = 2$ and higher harmonics $l = 3, 4$) is shown in Fig. 2.

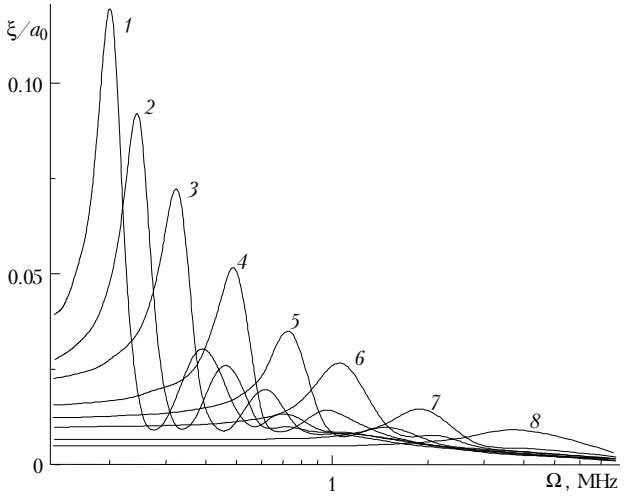

Fig. 1. Relative amplitude of steady oscillations vs. modulation frequency of acting radiation for droplets of different sizes: a_0 = 11.4 (*1*), 9.5 (*2*), 8.2 (*3*), 6.2 (*4*), 4.7 (*5*), 3.7 (*6*), 2.4 (*7*), and 1.6 μm (*8*).

The numerical analysis shows that these curves are well approximated by the power dependence $\sim a_0^{3/2}$. Some scatter of points is caused, first of all, by inhomogeneous distribution of the surface intensity of the electromagnetic field for optically large particles. Besides, the resonances in the internal optical field[12] can significantly increase the surface intensity of the electromagnetic field and, consequently, the amplitude of deformations.

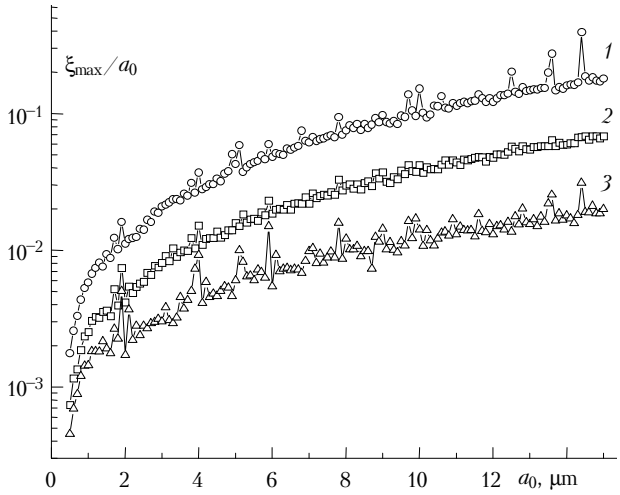

Fig. 2. Maximum relative amplitude of droplet oscillations vs. droplet size for different natural frequencies: Ω_2 (*1*), Ω_3 (*2*), and Ω_4 (*3*).

As an example, Fig. 3 shows the dependence of the radiation scattered by a group of particles on the modulation frequency of the pumping radiation. In this case, the standard gamma distribution is taken as a model particle size distribution function.

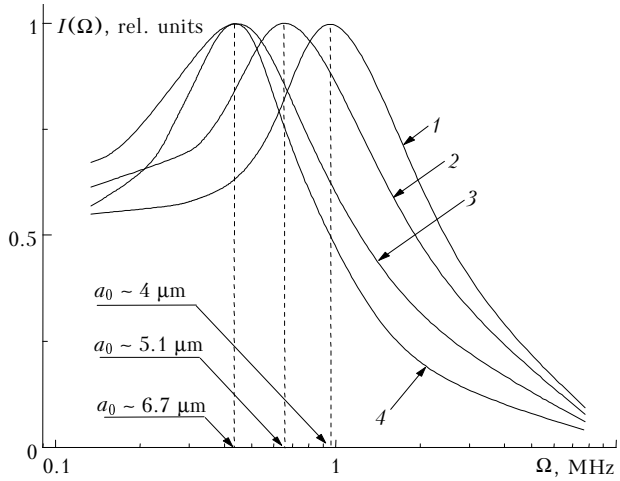

Fig. 3. Frequency dependence of the intensity of the radiation scattered by a group of particles for the initial gamma distributions with the following parameters: r_m = 3 μm and μ = 20 (*1*), r_m = 3 μm and μ = 10 (*2*), r_m = 3 μm and μ = 5 (*3*), r_m = 5 μm and μ = 20 (*4*). The frequency position of the intensity maxima and the corresponding particle sizes are shown.

At constant modal radius r_m and increasing halfwidth of the distribution μ, not only the halfwidth

of the frequency behavior of the scattered radiation intensity changes, but also the maximum itself shifts towards lower frequencies due to the increasing contribution of high frequencies to the scattering. Therefore, in actual experiments, the maximum in the frequency dependence of the scattered radiation falls on the frequency lower than that corresponding to the modal radius of the initial distribution. An exception is a monodisperse or nearly monodisperse distribution, for which these frequencies coincide. As a result, the maxima of the frequency behavior for two distributions with different halfwidths and modal radii can be observed at the same value of the modulation frequency (see Fig. 3, curves *3* and *4*). However, the halfwidths of these dependences are different. This points to the potential possibility of reconstructing the actual distribution by solving the inverse problem.

Thus, the frequency behavior of the amplitude of the low-frequency component of the radiation scattered by polydisperse aerosol carries information on the properties of the particle size distribution. However, obtaining the information on the particle size distribution function by direct recalculation of parameters from the frequency characteristic without solving the inverse problem is incorrect.

The principal diagonal of the matrix $I_s^i(\Omega_j)$ in Eq. (6) consists of the terms whose values are determined by the maxima in the frequency dependence of the oscillation amplitudes (see Fig. 1). However, because of the dependences shown in Fig. 2, this system is ill-posed, i.e., the determinant of the matrix $I_s^i(\Omega_j)$ is close to zero. To improve reconstruction, we should smooth the values in the principal diagonal. This can be done by the following procedure:

$$I(\Omega) = N_0\, V \int_0^\infty \frac{I_s(a_0,\, \Omega)}{a_0^s}\, a_0^s\, f(a_0)\, \mathrm{d}a_0, \qquad (7)$$

where s is the exponent chosen in the corresponding way.

The set of equations (6) with allowance made for Eq. (7) has been solved numerically with the use of standard IMSL libraries for FORTRAN 90 language (LSARG procedure) at $s = 1$. Besides this technique, the iterative algorithm proposed in Ref. 13 was used for solving the set (6). This simple algorithm is easily realizable with a computer. The distribution function at each iteration is converted in accordance with the equation

$$N_i^{p+1} = N_i^p\, I(\Omega_i) / I^p(\Omega_i),$$

where $I(\Omega_i)$ is the initial frequency dependence of the scattered radiation intensity; $I^p(\Omega_i)$ is the frequency dependence obtained with the use of the distribution function N_i^p at the pth iteration. The distribution functions reconstructed by the both methods gave close results, which are presented in Fig. 4. For the distributions shown in the figure, the frequency dependence maxima coincide, but the reconstruction allowed us to satisfactorily calculate the initial distribution functions.

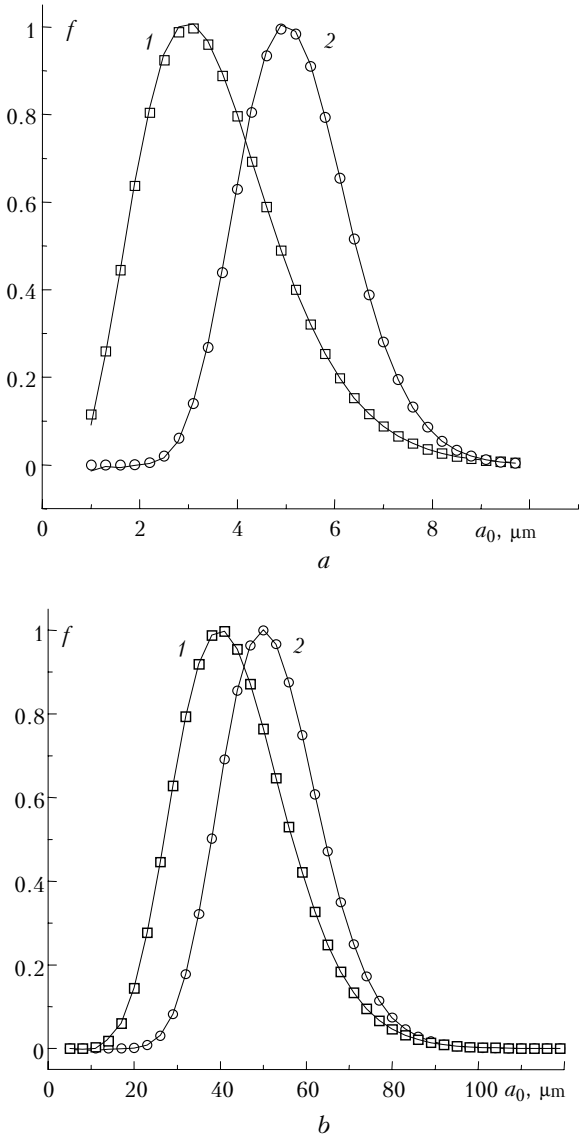

Fig. 4. Reconstructed distributions (curve) and model distribution (circles and squares); upper panel: r_m = 3 μm and μ = 5 (*1*), r_m = 5 μm and μ = 20 (*2*); lower panel: r_m = 40 μm and μ = 10 (*1*), r_m = 50 μm and μ = 20 (*2*).

An important problem is to estimate the stability of the solution, i.e., to analyze the influence of errors in the scattered radiation intensity on reconstruction of the distribution function. For random noise simulation, we used a random number generator of the IMSL procedures. Figure 5 shows the frequency behavior of the scattered radiation intensity. The vertical bars at three points show the root-mean-square (rms) scatter of the values averaged over ten samples. This scatter does not exceed 10% of the value of intensity at the given point. Figure 6 shows the model distribution,

reconstructed distribution for the problem free of noise, and averaged reconstructed distribution with noise in the frequency behavior, as well as the rms scatter at some points. In the region of larger sizes, the errors of reconstruction correspond to the errors in the frequency dependence. Although in the region of small sizes the errors of reconstruction are larger, averaging of the obtained distribution gives the result being sufficiently close to the initial distribution.

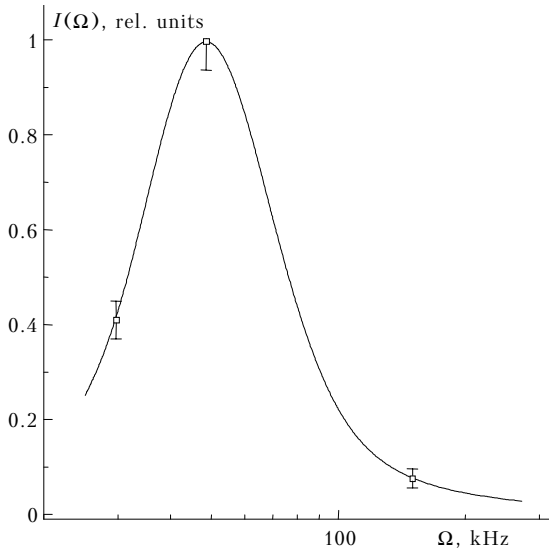

Fig. 5. Frequency characteristics of the intensity of scattered radiation in the model distribution (Fig. 6). The solid curve describes the initial dependence and the intensity value averaged over 10 samples under noise conditions; at three points the scatter of data is shown.

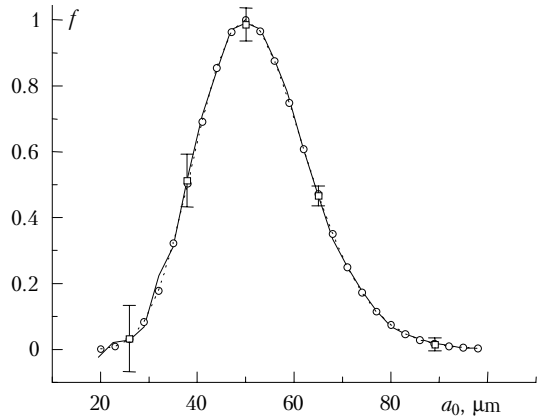

Fig. 6. Reconstructed distributions; the dashed line corresponds to the unperturbed problem, model distribution (open circles); the solid curve corresponds to the value averaged over 10 samples in the case of the noised frequency dependence (see Fig. 5); the scatter of the data is shown at some points.

The decrease of the modal radius in the model distributions leads to increase of the error of reconstruction. Thus, for the particle size $a_0 < 1$ μm the information on the initial distribution is lost almost completely because of blurring of the resonance dependence for such particles (see Fig. 1).

Conclusion

Solution of the inverse problem has allowed us to reconstruct the particle size distribution function with good accuracy. The analysis of solution stability has shown that for particles > 1 μm the reconstructed distribution function is stable to small errors in the frequency behavior of the scattered radiation intensity.

Thus, this research has demonstrated a possibility of practical application of the effect of dynamic light scattering at ponderomotive oscillations of droplet surface to reconstruction of the particle size distribution function of the liquid-droplet aerosol.

Acknowledgments

The authors are thankful to Dr. V.V. Veretennikov for valuable recommendations and criticism.

References

1. M. Brook and D.J. Latham, J. Geophys. Res. **73**, 7137–7144 (1968).
2. M. Brook and D.J. Latham, J. Atmospheric Sci. **32**, 2001–2007 (1975).
3. V.V. Sterlyadkin, Izv. Akad. Nauk SSSR, Ser. Fiz. Atmos. Okeana **24**, 613–621 (1988).
4. A.A. Zemlyanov, Kvant. Elektron. **1**, No. 9, 2085–2088 (1974).
5. Yu.A. Bykovskii, E.A. Manykin, et al., Kvant. Elektron. **3**, 157–162 (1976).
6. Yu.V. Ivanov and Yu.D. Kopytin, Kvant. Elektron. **9**, No. 3, 591–593 (1982).
7. A.A. Zemlyanov and Yu.E. Geints, Atmos. Oceanic Opt. **10**, Nos. 4–5, 313–321 (1997).
8. A.A. Zemlyanov, Yu.E. Geints, and A.V. Pal'chikov, Atmos. Oceanic Opt. **11**, No. 3, 819–825 (1998).
9. V.E. Zuev, A.A. Zemlyanov, Yu.D. Kopytin, and A.V. Kuzikovskii, *High-Power Laser Radiation in Atmospheric Aerosols* (D. Reidel Publ. Corp., Dordrecht, Holland, 1984), 291 pp.
10. L.D. Landau and E.M. Lifshitz, *Electrodynamics of Continuous Media* (Gostekhizdat, Moscow, 1957), 266 pp.
11. V.E. Zuev and I.E. Naats, *Current Problems of Atmospheric Optics*, Vol. 7 (Gidrometeoizdat, Leningrad, 1990), 287 pp.
12. A.A. Zemlyanov and Yu.E. Geints, Atmos. Oceanic Opt. **12**, No. 10, 895–904 (1999).
13. M.T. Chahine, J. Opt. Soc. Am. **58**, 1634–1637 (1968).